This article was downloaded by: [Ndubisi Aviara]
On: 05 April 2013, At: 10:28
Publisher: Taylor & Francis
Informa Ltd Registered in England and Wales Registered Number: 1072954 Registered office: Mortimer House, 37-41 Mortimer Street, London W1T 3JH, UK



Drying Technology: An International Journal
Publication details, including instructions for authors and subscription information:
http://www.tandfonline.com/loi/ldrt20

Influence of Cultivar on the Predictive Performance of a Moisture Transport Model Developed for Parboiled Paddy Drying

Lovelyn N. Onuoha [a], Ndubisi A. Aviara [b], Toyin A. Abdulrahim [a] & Ahmed T. Suleiman [c]
[a] Department of Mechanical Engineering, University of Maiduguri, Maiduguri, Nigeria
[b] Department of Agricultural and Environmental Resources Engineering, University of Maiduguri, Maiduguri, Nigeria
[c] Department of Mechanical Engineering, Bayero University, Kano, Nigeria
Version of record first published: 02 Apr 2013.

To cite this article: Lovelyn N. Onuoha , Ndubisi A. Aviara , Toyin A. Abdulrahim & Ahmed T. Suleiman (2013): Influence of Cultivar on the Predictive Performance of a Moisture Transport Model Developed for Parboiled Paddy Drying, Drying Technology: An International Journal, 31:5, 494-506

To link to this article: http://dx.doi.org/10.1080/07373937.2012.709206

PLEASE SCROLL DOWN FOR ARTICLE

Full terms and conditions of use: http://www.tandfonline.com/page/terms-and-conditions

This article may be used for research, teaching, and private study purposes. Any substantial or systematic reproduction, redistribution, reselling, loan, sub-licensing, systematic supply, or distribution in any form to anyone is expressly forbidden.

The publisher does not give any warranty express or implied or make any representation that the contents will be complete or accurate or up to date. The accuracy of any instructions, formulae, and drug doses should be independently verified with primary sources. The publisher shall not be liable for any loss, actions, claims, proceedings, demand, or costs or damages whatsoever or howsoever caused arising directly or indirectly in connection with or arising out of the use of this material.

Drying Technology, 31: 494–506, 2013
Copyright © 2013 Taylor & Francis Group, LLC
ISSN: 0737-3937 print/1532-2300 online
DOI: 10.1080/07373937.2012.709206

Taylor & Francis
Taylor & Francis Group

Influence of Cultivar on the Predictive Performance of a Moisture Transport Model Developed for Parboiled Paddy Drying

Lovelyn N. Onuoha,[1] Ndubisi A. Aviara,[2] Toyin A. Abdulrahim,[1] and Ahmed T. Suleiman[3]

[1]*Department of Mechanical Engineering, University of Maiduguri, Maiduguri, Nigeria*
[2]*Department of Agricultural and Environmental Resources Engineering, University of Maiduguri, Maiduguri, Nigeria*
[3]*Department of Mechanical Engineering, Bayero University, Kano, Nigeria*

Downloaded by [Ndubisi Aviara] at 10:28 05 April 2013

A mathematical model for predicting moisture profile in parboiled paddy during drying was developed using the prolate spheroidal coordinate system. The model was solved using the Crank Nicolson central difference scheme and the variation of its predictive potential with paddy cultivar was investigated. Parboiled paddy drying was carried out at 60°C using a cabinet tray dryer. The variation of the moisture ratio of different paddy cultivars (Banki, De-gold, and Liberia) with time and drying rate and with time and moisture content was determined. Model validation was carried out using residual plots, root mean square deviation, and coefficient of determination. The parboiled Banki, De-Gold, and Liberia paddy cultivars had equivalent diameters of 3.73, 4.75, and 3.68 mm, prolate spheroidal geometric dimensions (equatorial and polar radii) of 1.16 and 4.78 mm, 1.22 and 5.45 mm, and 3.10 and 3.92 mm, and effective moisture diffusion coefficient of 2.81934×10^{-10}, 5.71515×10^{-10}, and 3.77336×10^{-10} m^2/s, respectively. Drying of parboiled paddy occurred in the falling rate phase with initial period of induction and critical moisture content that varied with cultivar. The residual plots showed that the model was acceptable for predicting moisture transport in all the cultivars during drying. Comparison of the observed and predicted moisture ratios showed low root mean square deviation and high coefficient of determination, which varied with cultivar indicating that the predictive potential of the model was cultivar dependent.

Keywords Finite difference method; Mathematical model; Moisture diffusion; Parboiled paddy drying; Prolate spheroid

INTRODUCTION

Paddy is harvested rice that has been threshed to remove non-rice-grain materials. It is one of the leading food crops in the world with a total production of about 448 million metric tons of milled rice in the 2008/2009 production year.[1] In Nigeria, several varieties of the crop are commonly cultivated.[2] The grain is made up of an outer husk, a bran layer, and the endosperm (rice kernel). The husk layer accounts for 20% of the weight of the paddy and helps to protect the grain kernel from insect and fungal attack. Parboiled paddy is that which has been treated hydrothermally in the husk, to partially gelatinize the starch and harden the endosperm, making it translucent and more resistant to rodent, pest, and insect attack. Parboiling improves the milling recovery of paddy, salvages poor quality or spoiled paddy,[3] and causes certain nutritional and health benefits to accrue to the consumers.[4] The three operations involved in the parboiling process are soaking, steaming, and drying.[5] After the soaking and steaming operations, the paddy normally attains a moisture content of up to 60% (d.b.),[6] and such a high moisture condition that is not normally encountered in raw paddy processing[7] has to be reduced to the level needed for the commencement of milling. This makes drying a fundamental unit operation in parboiled paddy processing. Likitrattanaporn and Noomhorm[8] reported that simultaneous parboiling and drying of paddy by infrared heating had significant effect on milled rice quality. Since the rice kernel is fragile and sensitive to thermal and moisture stresses, the drying of the parboiled paddy requires different conditions and process control from that of the raw paddy.[9]

Accurate description and prediction of the drying behavior of grains are indispensable in the design of modern drying systems. A better insight into the moisture transport process taking place inside the kernel during drying can be obtained using appropriate mathematical models. Theoretical models based on Fick's second law of diffusion have been reported by several researchers.[7,10–14] The main

Correspondence: Ndubisi A. Aviara, Department of Agricultural and Environmental Resources Engineering, University of Maiduguri, Maiduguri, Nigeria; E-mail: nddyaviara@yahoo.com

Downloaded by [Ndubisi Aviara] at 10:28 05 April 2013

assumption that the heat transfer effects in the grain can be neglected and the process treated as a purely mass transfer one, with the main mechanism of moisture transport being diffusion, has been used with satisfactory results by investigators.[15,16] Parboiled paddy drying can therefore be considered as a process controlled by the migration of moisture in the grain where heat transfer effect can be neglected.[17] Another important consideration in modeling is the model geometry,[7] as this highly influences the accuracy of the predictions. In many theoretical drying models, the governing equation has been solved over an assumed standard geometry such as sphere,[18,19] slab,[20,21] and cylinder[22–24] with respect to initial and boundary conditions. If the assumed geometry is closer to the actual shape, the performance of the model will be better but the complexity will increase. De Lima and Nebra[25] and de Oliveira and de Lima[26] carried out theoretical analysis of moisture transfer process in prolate spheroidal solids using a constant diffusion coefficient and convective boundary condition, while Carmo and Lima[27] modeled mass transfer in oblate speroidal solids and Igathinathane et al.[28] utilized the prolate spheroidal coordinate system in modeling moisture diffusion during tempering in parboiled paddy. Prakash and Pan[29] noted that the type of shape assumed for the rice grain during modeling had a marked effect on the predictive performance of its drying models. The finite element method has been employed in the solution of diffusion problems, where the actual irregular shape was considered, in single component rice adsorption studies.[30,31] It was also employed by Sokhansanj and Gustafson,[32] Aguerre and Suarez,[33] Muthukumarappan and Gunasekaran,[34] Igathinathane and Chattopadhyay,[35] Rafiee et al.,[36] and Janas et al.[37] Complex shaped geometries are often modeled by the finite element method, and the method, though versatile in handling problems, is relatively difficult to apply. Igathinathane[38] simplified the computation in moisture diffusion modeling of paddy using prolate spheroid geometry and Igathinathane and Chattopadhyay[7,9] applied the prolate spheroidal coordinate system to the modeling of moisture diffusion in parboiled paddy. They, however, did not demonstrate the variation in the predictive capacity of the developed model with varietal differences.

The aim of this study was to develop a mathematical model for predicting moisture distribution and transport in parboiled paddy during drying. The specific objectives were: to apply the prolate spheroidal coordinates in modeling moisture movement in parboiled paddy during drying; validate the model using experimental drying data and such statistical tools as residual plots, root mean square deviation, and coefficient of determination; and investigate the response of the model to variation in parboiled paddy variety using the Banki, De-gold, and Liberia paddy cultivars.

DRYING MODEL DEVELOPMENT

Theoretical Basis of Model Formulation

The driving force of drying has been frequently considered to be moisture concentration gradient. In heated air drying, heating lowers the air relative humidity and, when it comes into contact with the moist material, the differential water vapor potential between the product and moist air is increased. This results in an overall mass diffusion as moisture then migrates from the region of high vapor pressure and moisture concentration to one of low vapor pressure and moisture concentration. Theoretical model equations involving a system of partial differential equations have been used to describe the heat and mass transfer processes inside cereal grains. Such a system of equations has been presented by Brooker et al.[19] as follows:

$$\frac{\partial M}{\partial t} = \nabla^2 \prec_{11} M + \nabla^2 \prec_{12} T + \nabla^2 \prec_{13} P \tag{1}$$

$$\frac{\partial T}{\partial t} = \nabla^2 \prec_{21} M + \nabla^2 \prec_{22} T + \nabla^2 \prec_{23} P \tag{2}$$

$$\frac{\partial P}{\partial t} = \nabla^2 \prec_{31} M + \nabla^2 \prec_{32} T + \nabla^2 \prec_{33} P \tag{3}$$

where M is moisture content (%), T is temperature (°C) and P is pressure (Pa), $\prec_{11}$, $\prec_{22}$, *and* $\prec_{33}$ are phenomenological coefficients, while the other $\prec$-values represent the coupling coefficients. Moisture flow due to total pressure gradient is significant only in drying at product temperature well above the temperature range normally employed in cerealgrain drying.[19] This means that the pressure terms can be dropped, thus the modified system of equations describing grain drying becomes:

$$\frac{\partial M}{\partial t} = \nabla^2 \prec_{11} M + \nabla^2 \prec_{12} T \tag{4}$$

$$\frac{\partial T}{\partial t} = \nabla^2 \prec_{21} M + \nabla^2 \prec_{22} T \tag{5}$$

The coupling effects of temperature and moisture in the analysis of cerealgrain drying are negligible; therefore, the phenomenological equations become[19]:

$$\frac{\partial M}{\partial t} = \nabla^2 \prec_{11} M \tag{6}$$

$$\frac{\partial T}{\partial t} = \nabla^2 \prec_{22} T \tag{7}$$

Eqs. (6) and (7) describe the moisture and thermal transfer in the grains during drying. The phenomenological transfer coefficients $\prec_{11}$ *and* $\prec_{22}$ are the moisture diffusivity "D" and thermal diffusivity "α", respectively. Eqs. (6) and (7)

Downloaded by [Ndubisi Aviara] at 10:28 05 April 2013

could therefore be taken as the Laplacian expressions of Fick's law of diffusion in which concentration is replaced with its analogous quantity called moisture[26,27] and Fourier's law of heat transfer in which temperature replaced the heat per unit volume, respectively, in terms of time in various coordinates. ∇ is the Del operator. Hence, the Fick's law of diffusion and Fourier's law of heat conduction in terms of time in a given coordinate can be stated as follows:

$$\left(\frac{\partial M}{\partial t}\right)_x = -D\frac{\partial M}{\partial x} \tag{8}$$

$$\left(\frac{\partial T}{\partial t}\right)_x = -\alpha\frac{\partial T}{\partial x} \tag{9}$$

In practical analysis of cereal grain drying, temperature gradient can be neglected.[19] Thus, temperature transport within the samples was neglected and Eq. (8) became the equation upon which the model development was based.

Drying Model Formulation

Brooker et al.[19] gave a solution to Eq. (8) for predicting the drying behavior of cereal grains as:

$$\frac{\partial M}{\partial t} = D\left[\frac{\partial^2 M}{\partial r^2} + \frac{\mathbb{C}}{r}\frac{\partial M}{\partial r}\right] \tag{10}$$

where $\mathbb{C}$ is zero for planar geometry, unity for a cylindrical body, and two for spheres. These solutions could not be applied to the analysis of paddy drying as the grain has been generally described as a prolate spheroid.[7,9,26,28] The prolate spheroidal coordinate system was therefore used to simplify the computation in the mass transfer modeling of parboiled paddy during drying. The following assumptions were made in the model development:

- Moisture distribution within parboiled paddy grains is uniform at the beginning of the drying process.
- The only mechanism of moisture transport inside the solid is vapor diffusion.
- The drying air is distributed uniformly through the drying system.
- There is negligible shrinkage or deformation of the paddy grain.

The prolate spheroid characteristics are shown in Fig. 1.

L is the focal length given as

$$L = (L_2^2 - L_1^2)^{1/2} \tag{11}$$

where L_1 is the equatorial radius and L_2 is the polar radius. Any point in the prolate spheroidal coordinate system (Fig. 1) can be represented by the values of the coordinates

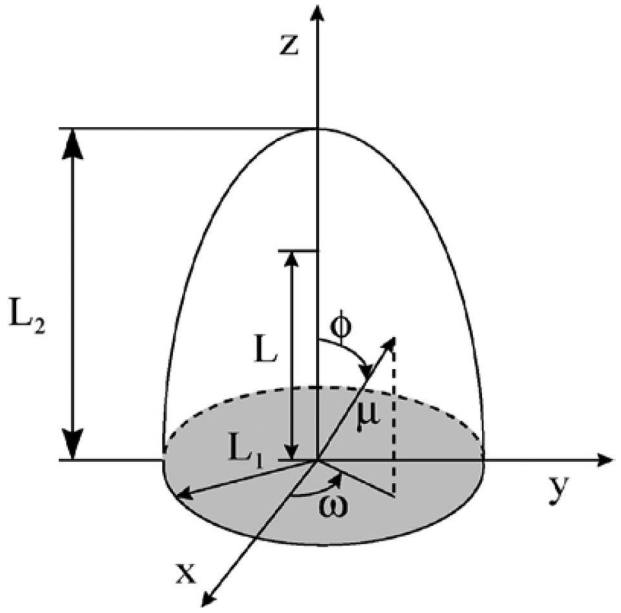


FIG. 1. Characteristics of a prolate spheroidal solid.[25]

as (μ, ϕ, ω). The relations between the Cartesian (x, y, z) and the prolate spheroidal (μ, ϕ, ω) coordinate systems are[26]:

$$\left.\begin{aligned} x &= L\sinh\mu\sin\phi\cos\omega \\ y &= L\sinh\mu\sin\phi\sin\omega \\ z &= L\cosh\mu\cos\phi \end{aligned}\right\} \tag{12}$$

The ranges of values for the prolate spheroidal co-ordinates are $0 \le \mu < \infty$, $0 \le \phi \le \pi$ *and* $0 \le \omega \le 2\pi$. μ is the distance apart from the origin and a point on the prolate spheroidal confocal surface, ϕ is the angle of inclination to the z-axis of the hyperbola lines. ω is the azimuth angle.

Isolating an elemental portion from the orthogonal grids in aprolate spheroid and, considering moisture transfer within the particle along the axes represented by Eq. (12) using the Laplacian expression of the governing Eq. (10), the following expression was obtained.

$$\frac{1}{D}\frac{\partial^2 M}{\partial t^2} = \frac{\partial^2 M}{\partial(L\sinh\mu\sin\phi\cos\omega)^2} + \frac{\partial^2 M}{\partial(L\sinh\mu\sin\phi\sin\omega)^2} + \frac{\partial^2 M}{\partial(L\cos\ h\mu\cos\phi)^2} \tag{13}$$

Taking $\xi = \cosh\mu$, $\eta = \cos\phi$ and $\zeta = \cos\omega$, a new prolate spheroid coordinate system[26] was established as shown in Fig. 2.

ξ defines the confocal prolate lines and they have their common center at the origin. $\xi > 1$ is an elongated ellipsoid of revolution with polar axis of length $L\xi$ and equatorial length axis $L(\xi^2 - 1)^{1/2}$. The degenerate surface $\xi = 1$ is

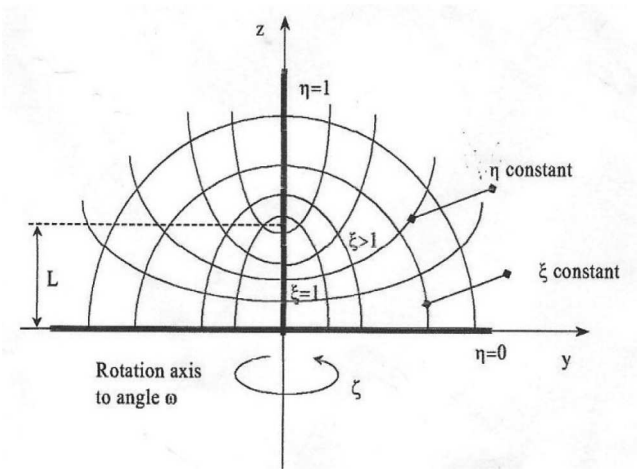


FIG. 2. New prolate spheroidal coordinate system.

the curve that links the center (z = 0) to the focal point (z = L). η defines the confocal hyperbola lines intersecting the entire family of prolate spheroids orthogonally. Utilizing the variables ξ, η, and ζ and the differentiation rules, Eq. (13) becomes:

$$\frac{\partial M}{\partial t} = \left[\frac{1}{L^2(\xi^2-\eta^2)}\frac{\partial}{\partial \xi}\left((\xi^2-1)D\frac{\partial M}{\partial \xi}\right)\right] + \left[\frac{1}{L^2(\xi^2-\eta^2)}\frac{\partial}{\partial \eta}\left((1-\eta^2)D\frac{\partial M}{\partial \eta}\right)\right] + \left[\frac{\sqrt{1-\zeta^2}}{L^2(\xi^2-1)(1-\eta^2)}\frac{\partial}{\partial \zeta}\left(\left(\sqrt{1-\zeta^2}\right)D\frac{\partial M}{\partial \zeta}\right)\right] \quad (14)$$

The coordinates (ξ, η, ζ) range as $0 \le \xi < \infty$, $0 \le \eta \le \pi$, and $0 \le \zeta \le 2\pi$. For a symmetric field of moisture around the z-axis, a new set of variables (ξ, η, t) was obtained with coordinates range of $0 \le \xi < \infty$, $0 \le \eta \le \pi$ and $0 \le t \le \infty$. Eq. (14) becomes:

$$\frac{\partial M}{\partial t} = \left[\frac{1}{L^2(\xi^2-\eta^2)}\frac{\partial}{\partial \xi}\left((\xi^2-1)D\frac{\partial M}{\partial \xi}\right)\right] + \left[\frac{1}{L^2(\xi^2-\eta^2)}\frac{\partial}{\partial \eta}\left((1-\eta^2)D\frac{\partial M}{\partial \eta}\right)\right] \quad (15)$$

Using the method of separation of variables in a multi-dimensional prolate system, a product solution of the form due to Kreyzig[39] was assumed such that the function for M (moisture) became

$$M(\xi_f, \eta, t) = \mathrm{f}(\xi_\mathrm{f})\mathbb{h}(\eta)\mathfrak{G}(\mathrm{t}) \quad (17)$$

The mass diffusion model was then initiated using the following considerations:

$$\mathrm{M}\,|_{\mathrm{t}=0} = \mathrm{M_i} \quad (18)$$

For $t > 0$

$$-\frac{D}{L}\sqrt{\frac{(\xi^2-1)}{(\xi^2-\eta^2)}}\frac{\partial M}{\partial \xi}\bigg|_{\xi=\xi_f} = h_m\left[M(\xi=\xi_f,\eta,t) - M_e\right] \quad (19)$$

Under a given drying condition the minimum moisture content to which the grain can be dried is called the equilibrium moisture content, M_e. Thus,

$$\text{for } \xi = 0 : M(0,\eta,t) = 0 \textit{ and for } \xi = \xi_f . M(\xi_f,\eta,t) = h_m(M - M_e) \quad (20)$$

$$\text{for } \eta = 0 : M(\xi,0,t) = h_m(M - M_e) \textit{and for } \eta = \eta : M(\xi,\eta,t) = h_m(M - M_e) \quad (21)$$

$$\textit{and for all } t : M(\xi,\eta,\mathrm{t}) = G(\xi) = h_m(M - M_e) \quad (22)$$

where h_m is mass transfer coefficient, ξ_f is L_2/L at the surface of the solid, M is dry basis moisture content (kg of H_2O/kg of Dry Matter (D.M)), M_i is initial moisture content (kg of H_2O/kg of D.M), M_e is final or equilibrium moisture content (kg of H_2O/kg of D.M), and t is time (s).

Let ξ represent the equipotential prolate spheroidal surface having the same moisture content values, while η represents the field line on the hyperboloidal surface along which the moisture content gradients develop. Since the prolate spheroid geometry is symmetrical, an appropriate selection of ϕ value and evaluation of the moisture gradients along the x-axis reduced the three-dimensional model equation (14) through Eq. (15) to a one-dimensional equation, which according to Igathinathane and Chattopadhyay[7] produced the same results. The workable 1-D mass diffusion model in the prolate spheroidal coordinate system for drying parboiled paddy therefore becomes:

$$\frac{\partial M^{\blacksquare}}{\partial t} = \frac{D}{L^2\xi^2}\left[2\xi\left(\frac{\partial M^{\blacksquare}}{\partial \xi}\right) + (\xi^2-1)\left(\frac{\partial M^{\blacksquare}}{\partial \xi^2}\right)\right] \quad (23)$$

$M^{\blacksquare}$ is 1-D moisture content (kg/kg).

Non-Dimensionalization of Model Equation

The data involving moisture content of parboiled paddy during drying were transformed into dimensionless moisture ratios.[40] The dimensionless moisture (M^*) was expressed as

$$M^* = \frac{M - M_e}{M_i - M_e} \quad (24)$$

Downloaded by [Ndubisi Aviara] at 10:28 05 April 2013

Downloaded by [Ndubisi Aviara] at 10:28 05 April 2013

The dimensionless model equation was obtained by substituting the following set of dimensionless parameters into Eq. (23) and simplifying.

$$\text{(i) } M^* = \frac{M^{\blacksquare} - M_e^{\blacksquare}}{M_i^{\blacksquare} - M_e^{\blacksquare}} \quad \text{(ii) } F_{o_m} = \frac{Dt}{L_c^2} \quad \text{(iii) } D^* = \frac{D}{D} \tag{25}$$

F_{o_m} is the mass transfer Fourier number, L_c is the characteristic length of the paddy (focal length, L (mm)). D^* is the dimensionless diffusion coefficient of sample material with respect to itself while t (s) is time. This yielded the dimensionless 1-D prolate spheroidal model equation as:

$$\frac{\partial M^*}{\partial F_{o_m}} = \frac{D^*}{\xi^2}\left[2\xi\left(\frac{\partial M^*}{\partial \xi}\right) + \left(\xi^2 - 1\right)\left(\frac{\partial M^*}{\partial \xi^2}\right)\right] \tag{26}$$

Dimensionless Domain Grid Generation

To solve Eq. (26) using the finite difference method, the paddy geometry was divided into grids as shown in Fig. 3. The specific direction of the ξ-axis was chosen where $\phi = \pi/2$ and $\omega = 0$ for laying out the nodes to form the 1-D grid scheme. The nodes were evenly spaced along the ξ-axis.

The boundary conditions became:

Initial Condition

All the nodes are at the initial moisture content so

$$F_{o_m} = 0; \qquad \xi \le 10h'; \qquad M^* = 1.0 \tag{27}$$

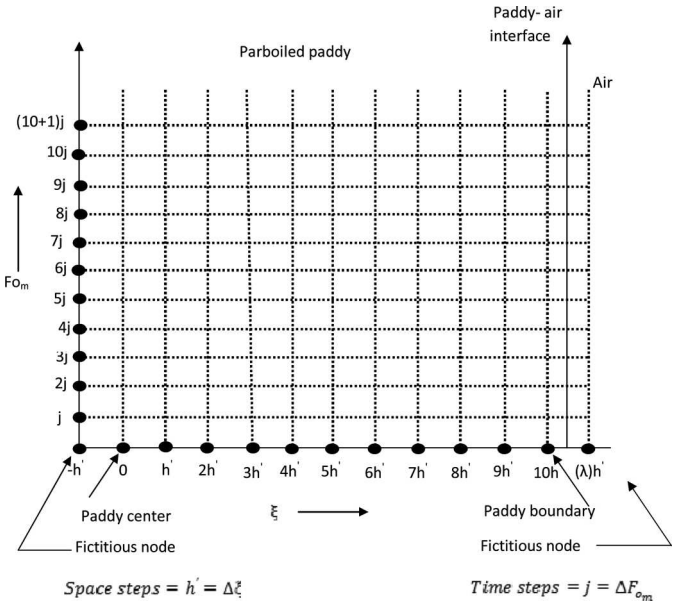


FIG. 3. Layout of nodes and dimensionless grid scheme of the moisture transfer model.

Boundary Conditions

(a) At the center of the paddy sample

$$F_{o_m} > 0; \ \xi = 1.0; \ \frac{\partial M^*}{\partial \xi} = 0 \tag{28}$$

The paddy geometry was considered symmetric at the center and the moisture ratio at both sides of the center node was taken to be equal, thereby making the moisture gradient equal to zero.

(b) At the paddy sample surface (surface-air interface)

$$F_{o_m} > 0; \quad \xi = 10h'; \quad \frac{-\partial M^*}{\partial \xi} = Bi_m M^* \tag{29}$$

where

$$Bi_m = \frac{h_m L_c}{D} \tag{30}$$

D = mass diffusivity (m^2/s), h_m = mass transfer coefficient (kg mol/m^2s Pa),

L_c = characteristic length of the paddy (focal length) (m).

The function of the mass transfer Biot number was to cause a realistic gradual decrease in the moisture content of the boundary node to the final moisture content. The h_m of parboiled paddy was obtained from Rao et al.[41] The moisture sorption isotherm slope of parboiled paddy in kg/m^3 Pa was used to normalize the mass transfer biot number into a dimensionless variable because of the h_m dimension.[7]

Finite Difference Equations of the Drying Model

The finite difference equations of the drying model (Eq. (26)) with the application of Eqs. (27) to (30) were derived using the Crank-Nicolson's central difference scheme[7,9,42,43] for the different regions of the geometry and are as explained below.

Middle Region of Paddy Sample

The nodes in the middle region of Fig. 3 were considered surrounded by nodes of similar nature. The finite difference equation of this region was based on Eq. (26) and the expansion using the Crank-Nicolson's scheme is given in Eq. (31)

$$\begin{aligned}\frac{M_i^{*\prime} - M_i^*}{j} &= \frac{D^*}{\xi_i^2}\left\{(2\xi_i)\frac{1}{2}\left[\left(\frac{M_{i+1}^{*\prime} - M_{i-1}^{*\prime}}{2h'}\right) + \left(\frac{M_{i+1}^* - M_{i-1}^*}{2h'}\right)\right]\right. \\ &\quad + \left(\xi_i^2 - 1\right)\frac{1}{2}\left[\left(\frac{M_{i+1}^{*\prime} - 2M_{i-1}^{*\prime}}{h'2}\right)\right. \\ &\quad \left.\left. + \left(\frac{M_{i+1}^* - 2M_i^* + M_{i-1}^*}{h'2}\right)\right]\right\}\end{aligned} \tag{31}$$

M^* is the moisture ratio of present time step at F_{o_m} and $M^{*\prime}$ is the moisture ratio of a future time step at $F_{o_m} + F_{o_m}$, and i is the node index. Grouping terms of the same time step yielded the following generalized equation, which was applied to all the regions of the geometry with modifications:

$$\begin{aligned} &M^{*\prime}_{i-1}(\mathfrak{C} - \&) + M^{*\prime}_{i}(1 + 2\&) + M^{*\prime}_{i+1}(-\mathfrak{C} -) \\ &\quad = M^{*}_{i-1}(-\mathfrak{C} +) + M^{*}_{i}(1 - 2\&) + M^{*}_{i+1}(\mathfrak{C} +) \end{aligned} \tag{32}$$

where

$$\mathfrak{C} = \frac{jD^*}{2\xi_i^h} \text{ and } \& = \frac{jD^*\left(\xi_i^2 - 1\right)}{2\xi_i^2 h^2} \tag{33}$$

For the middle region, $0 < i < \lambda - 1$.

Center of Sample

At the center of the sample, $i = 0$, $\xi_i = 1$.

The finite difference equation common to the space steps on both sides of the center node based on Eq. (28) is

$$\frac{M^*_{i-1} - M^*_{i+1}}{2h'} = 0 \tag{34}$$

which yielded

$$M^*_{i-1} = M^*_{i+1} \tag{35}$$

Substituting Eq. (35) in the general finite difference equation (32) and replacing the M^*_{i-1} term, which is a fictitious or auxiliary moisture ratio, and simplifying gives

$$M^*_i(1 + 2\&) + M^*_{i+1}(-2\&) = M^*_i(1 - 2\&) + M^*_{i+1}(+2\&) \tag{36}$$

Paddy Sample Surface (Paddy Surface-Air Interface)

The paddy surface is the last node where $i = 10 = \lambda - 1$. The paddy surface-air interface is aligned between the nodes $\lambda - 1$ and λ, and the finite difference equation common to both space steps based on the boundary condition equation (29) was obtained as:

$$\frac{M^{*\prime}_{\lambda} - M^{*\prime}_{\lambda-1}}{h'} = -\frac{Bi}{2}\left(M^{*\prime}_{\lambda} + M^{*\prime}_{\lambda-1}\right) \tag{37}$$

On simplification, Eq. (37) becomes

$$M^{*\prime}_{\lambda} = \left(\frac{2 - Bih'}{2 + Bih'}\right) M^{*\prime}_{\lambda-1} \tag{38}$$

Substituting for the fictitious variable $M^{*\prime}_{\lambda}$ in Eq. (32) and simplifying yielded

$$\begin{aligned} &M^{*\prime}_{\lambda-2}(\mathfrak{C} - \&) + M^{*\prime}_{\lambda-1}\left[1 + 2\& - (\mathfrak{C} + \&)\left(\frac{2 - Bih'}{2 + Bih'}\right)\right] \\ &= M^{*}_{\lambda-2}(-\mathfrak{C} + \&) + M^{*}_{\lambda-1}\left[1 - 2\& + (\mathfrak{C} + \&)\left(\frac{2 - Bih'}{2 + Bih'}\right)\right] \end{aligned} \tag{39}$$

The finite difference equations (32) to (39) produced a system of algebraic equations, which were solved for the values of $M^{*\prime}$ at different nodes from the values of M^* corresponding to the preceding time step. The algebraic equations were conveniently represented by matrix notation. It was observed that the coefficient matrix was tridiagonal. This enabled the standard numerical algorithm of Guassian elimination to be applied to the model solution. The nodes were considered to be surrounded by two prolate spheroidal surfaces, each $h'/2$ away from the node, and the moisture content of the node is the representative value of the resulting elemental volume between the surfaces. For a node i, the ξ values of the elemental volume are $\xi_{i-h'/2}$ and $\xi_{i+h'/2}$. The total volume up to the left side of the prolate spheroidal surface of the node is:[7]

$$V_{i-h/2} = \frac{4}{3}\pi L^3 \xi_{i-h/2}\left(\xi^2_{i+h/2} - 1\right) \tag{40}$$

The elemental volume of the prolate spheroid corresponding to the ith node $\left(V_i^{\blacksquare}\right)$ enclosed by the two prolate spheroidal surfaces was obtained from the difference of the total volumes as:

$$\begin{aligned} V_i^{\blacksquare} &= V_{i+h'/2} - V_{i-h'/2} \\ &= \frac{4}{3}\pi L^3\left[\left(\xi^3_{i+h'/2} - \xi^3_{i-h'/2}\right) - \left(\xi_{i+h'/2} - \xi_{i-h'/2}\right)\right] \end{aligned} \tag{41}$$

The total moisture ratio (MR) of the whole paddy geometry was obtained by integrating the nodal M^*_i values applied to the individual volume of the elemental layers between suitable limits as:

$$MR = \frac{1}{V_{ps}}\left[V_{h'/2}M_{cn} + \sum_{i=1}^{\lambda-1}\left(V_i^{\blacksquare}M^*_i\right)\right] \tag{42}$$

where V_{ps} is the volume of the whole paddy grain, $V_{h'/2}$ is the volume enclosing the node at the center of the geometry, and M_{cn} is the moisture ratio of the central node.

In the drying model, the only unknown is the moisture diffusion coefficient of parboiled paddy grain (D). The diffusion coefficient, taken as the effective moisture diffusion

Downloaded by [Ndubisi Aviara] at 10:28 05 April 2013

coefficient, was determined from thin layer drying experiments carried out using a cabinet tray dryer. The plot of Ln(MR) against time (t) yielded a straight line with slope as[44]:

$$-B = -\frac{\pi^2 D}{r^2} \tag{43}$$

where r (m) is the equivalent radius.

MATERIALS AND METHODS

Sample Collection and Preparation

Sample Collection

The three paddy accessions used in testing the drying model and investigating the influence of cultivar on its predictive performance were the Banki, De-gold, and Liberia. These paddy cultivars were sourced from Biu and Banki Local Government Areas of Borno State, Nigeria. The samples were less than six months from the date of harvest at the time of purchase. Samples of the three cultivars are shown in Figs. 4 to 6, respectively.

Sample Preparation

The paddy samples were parboiled and prepared for drying tests by soaking and steaming as follows:

Soaking: This operation was carried out using the technique of Miah et al.[5] Each sample of the three paddy cultivars was soaked in hot water at a temperature of 80°C for 2 h to increase their moisture content. Free water was drained off and the sample surface was maintained water-free.



FIG. 5. De Gold paddy cultivar (color figure available online).

Steaming: Following the methods of Ibukun,[3] the soaked samples were steamed at 100°C for 15 min to further gelatinize the starchy content, after which they were tempered until all the liquid water was lost and the samples' surfaces were free of water. This enabled the samples to cool and moisture to be uniformly distributed.[2] The initial moisture contents of the samples were then determined by oven drying at 105°C for 6 h.[45]



FIG. 4. Bankipaddy cultivar (color figure available online).



FIG. 6. Liberia paddy cultivar (color figure available online).

Downloaded by [Ndubisi Aviara] at 10:28 05 April 2013

Downloaded by [Ndubisi Aviara] at 10:28 05 April 2013

Physical Properties of Parboiled Paddy

The axial dimensions with which the prolate spheroidal geometry and coordinates were established, namely length, width, and thickness of the parboiled paddy cultivars (Banki at 37.14%, De gold at 40%, and Liberia at 29.28% wet basis moisture content), were determined using a verniercalliper, (Supertek C-3823, England) reading to 0.1 mm. One hundred randomly selected grains from each parboiled sample were used. The equivalent diameter (D_e) and volume (V_e) considering prolate spheroid as the shape of the paddy grains were calculated using Eqs. (44) and (45) due to Reddy and Chakraverty[46] and Kibar et al.,[47] respectively:

$$D_e = \left[4l_i\left(\frac{w_i + t_i}{4}\right)^2\right]^{1/3} \tag{44}$$

$$V_e = \frac{\pi(w_i t_i)^{0.5} l_i^2}{6\left[2l_i - (w_i t_i)^{0.5}\right]} \tag{45}$$

where

l_i, W_i and t_i are the length, width, and thickness (m), respectively, and "a" and "c" are the equatorial and polar radii of the prolate spheroid. The aspect ratio of the samples was determined and their sphericity ø calculated using Eq. (46).

$$ø = \frac{(l_i w_i t_i)^{1/3}}{l_i} \tag{46}$$

From the measured axial dimensions and based on equivalent volume consideration, the prolate spheroid geometry dimensions "a" and "c" of the samples were obtained using Eqs. (47) and (48), respectively.[7]

$$a = \left(\frac{1}{2}\right)\sqrt{\left(\frac{w_i^2 + t_i^2}{2}\right)} \tag{47}$$

$$c = \frac{l_i w_i t_i}{w_i^2 + t_i^2} \tag{48}$$

Drying Tests and Model Validation Procedure

The drying of parboiled paddy samples for model verification was carried out using a cabinet tray dryer at a drying temperature of 60°C. The procedure employed by Syrarief et al.[48] and Ajibola[49] was adopted with modifications to suit the experimental condition. For a drying run to commence, the fuel in a reactor combustion chamber was ignited, allowed to burn and produce heat. Ambient air at average temperature of 35°C and 40% relative humidity was aspirated through the reactor and air flow tunnel into the drying chamber using a blower. The thermostatically controlled dryer was allowed to run empty for about 30 minutes to enable it to stabilize at the preset drying air condition. The initial moisture contents of the samples were then noted.

Triplicate samples of a given parboiled paddy, each weighing 30 g, were spread on a sample basket in a thin layer and placed on the drying bed. Change in sample weight was monitored throughout the experiment by weighing periodically using an electronic balance. Weighing of samples was carried out every 10 min for the first 1 h. Weighing was continued at intervals of 20 min until three consecutive readings gave identical weights. The test was then terminated, the time taken was recorded, and equilibrium with the drying environment assumed to have been reached. The samples at this point were oven dried at 105°C for 6 h[45] and their moisture contents were determined.

The moisture contents obtained with time for each sample were used to compute the moisture ratios that were used to validate the developed model. The experimental and predicted moisture ratios were plotted against time and compared to determine the predictive capacity of the model using residual plots, root mean square deviation (RMSD), and coefficient of determination (R^2). A model is considered acceptable if the residuals were uniformly scattered around the horizontal value of zero showing no systematic tendencies towards a clear pattern.[50] A model is considered to give a good fit if the coefficient of determination is high and close to 1.0, while the root mean square deviation is low. The parameters were computed using Eqs. (49) and (50)[28,51]:

$$RMSD = \sqrt{\frac{\sum_1^N \left(MR_{obs} - MR_{pred}\right)^2}{N}} \tag{49}$$

$$R^2 = \left(1 - \frac{\sum\left(MR_{obs} - MR_{pred}\right)^2}{\sum\left(MR_{obs} - MR_{mean}\right)^2}\right) \tag{50}$$

where

MR_{obs} and MR_{pred} are observed and predicted moisture ratio values, respectively, N is the number of observation in each set, and MR_{mean} is the mean of the observed moisture ratio values.

RESULTS AND DISCUSSION

Physical Properties of Parboiled Paddy

The axial dimensions, aspect ratio, equivalent diameter and volume, and sphericity of parboiled Banki, De-gold, and Liberia paddy cultivars at specified moisture content are presented in Table 1. The average length, width, and thickness of the samples showed that the De-gold was longer than the others. The Liberia cultivar had the largest

TABLE 1
Physical properties of parboiled paddy cultivars

Sample	Moisture content, %	Length l_i (mm)	Width w_i (mm)	Thickness t_i (mm)	Aspect ratio, w_i/l_i	Equivalent diameter D_e (mm)	Equivalent volume, V_e (mm^3)	Sphericity, ø (%)
Banki	37.14	9.86 (0.63)*	2.59 (0.22)	2.02 (0.16)	0.26 (0.03)	3.73 (0.24)	27.014 (1.42)	37.29 (1.72)
De Gold	40	11.21 (0.56)	2.70 (0.19)	2.13 (0.23)	0.24 (0.02)	4.75 (1.73)	33.76 (1.51)	35.26 (2.36)
Liberia	29.28	8.32 (0.43)	2.88 (0.29)	2.03 (0.05)	0.35 (0.03)	3.68 (0.19)	25.47 (1.37)	42.95 (1.84)

*Numbers in parentheses are standard deviations.

aspect ratio and the sphericity of the samples was generally below 50%, with the Liberia having the highest value. This was an indication that the grains should not be referred to as spheres and proved that the Liberia was of the medium-grain type (Table 2) while the Banki and De-gold were of the slender type.

Prolate Spheroid Geometry Dimensions of Parboiled Paddy Cultivars

From parboiled paddy axial dimensions, the prolate spheroid equatorial "a" and polar "c" radii were obtained and are presented in Table 2. Polar radius was generally larger than equatorial radius. This confirmed the parboiled paddy grains to be prolate spheroids. The Liberia had the largest equatorial radius, while the De-gold had the longest polar radius. This further points to the reason why the Banki and De-gold both had a slender prolate shape while the Liberia had a medium prolate shape.

Drying Model Validation

The solution of the 1-D prolate dimensionless model (Eq.(26)) using a Crank Nicolson central difference scheme and considering the initial and boundary conditions yielded the dimensionless moisture ratio at each node of the prolate spheroidal grid formed and the moisture ratio at the last node (paddy surface). Considering the equatorial radius value "a" of each paddy cultivar with node allotment done along the ξ - axis using a space step (h') value of 0.0031, 0.003, and 0.0634 for the Banki, De-gold, and Liberia samples, respectively, 10 grid nodes were formed for each sample. Effective moisture diffusivities of the samples were obtained from the experimental drying data and used to calculate the mass transfer Fourier number, while change in the mass transfer Fourier number gave the time step "j" (Table 3) for grid allotment.

Experimental drying was carried out with parboiled paddy samples at initial wet basis moisture contents of 37% (Banki), 40% (De-gold), and 29% (Liberia), respectively. The effective moisture diffusion coefficient obtained for each sample is presented in Table 3. Its value was found to be within the range of 10^{-11} to $10^{-9}\,m^2/s$, generally considered acceptable for agricultural and food products.[52] The moisture diffusion coefficient of the Banki cultivar was higher than that of De-gold and Liberia. The mass transfer coefficient used in determining the mass transfer Biot number was obtained from Rao et al.[41] Moisture sorption isotherm slope of parboiled paddy was used to normalize the mass transfer Biot number into a dimensionless variable because of the h_m dimension.[7] The characteristic length used was the focal length of each sample, given as 4.637 mm, 5.312 mm, and 2.399 mm for the Banki, De-gold, and Liberia, respectively. Eq. (42) gave the model predicted moisture ratio of the whole sample.

The plots of moisture profile in parboiled paddy samples during drying at 60°C (not presented here) showed that the moisture ratio of the boundary node of each cultivar reduced rapidly and approached the moisture ratio corresponding to the equilibrium moisture content. This was in agreement with the findings of Igathinathane and Chattopadhyay.[7] From 0.2 h onwards an inclined but fairly linear profile was observed. At the end of drying, the resulting profile indicated that all the nodes in the geometry reached the equilibrium moisture content corresponding to the drying air conditions.

The experimental drying data (Table 3) was used to validate the model and the validity was confirmed using

TABLE 2
Prolate spheroidal geometric dimensions of parboiled paddy cultivars

Paddy cultivar sample	Polar radius c (mm)	Equatorial radius a = b (mm)	Prolate shape	Grain type
Banki	4.78	1.16	slender	Long
De Gold	5.45	1.22	slender	Long
Liberia	3.92	3.10	medium	Medium

Downloaded by [Ndubisi Aviara] at 10:28 05 April 2013

TABLE 3
Drying data and model performance assessment parameters for parboiled paddy cultivars

Paddy sample	Temperature (°C)	Time step (j)	Diffusion coefficient (m^2/s)	EMC %	Statistical analysis	
					RSMD	R^2
Banki	60	5.3102×10^{-3}	2.81934×10^{-10}	6.10	0.013767	0.999136
De Gold	60	7.2923×10^{-3}	5.71515×10^{-10}	7.28	0.02104	0.999764
Liberia	60	2.35981×10^{-3}	3.77336×10^{-10}	6.76	0.030098	0.999465

residual plots (Fig. 7), RMSD, and R^2 values. From Table 3, it can be seen that the dynamic equilibrium moisture content (EMC) of parboiled paddy dried at the temperature of 60°C varied with cultivar. Of the three samples, the De-gold cultivar had the highest equilibrium moisture content. Residual plots are plots of the difference between the observed and predicted moisture ratios (MR_{Obs}-MR_{Pred}), against the observed moisture ratios (MR_{Obs}). These plots were found to be uniformly scattered about the x-axis, depicting that the model did not show a tendency towards a clear pattern. Therefore, the model could be said to be acceptable for predicting moisture migration in parboiled paddy during drying. A comparison of the residual plots shows that the shape varied with paddy cultivar, indicating that the predictive performance of the model could be cultivar-dependent.

The RMSD and R^2 obtained from the evaluation of the developed model on the drying data of each paddy cultivar are shown in Table 3. RMSD is the root mean of the sum of the squared deviation between the predicted and experimental moisture ratios. The lower the RMSD value, the more accurate would be the prediction of the model, and it was less than 0.04 for all the cultivars. The Banki cultivar had the lowest value of RMSD while the Liberia had the highest value. The R^2 measured the performance of the model on the trend of the moisture ratio with time and was found to be more than 0.999 for all the samples, reflecting good agreement between the predicted and observed values. The Liberia cultivar had the highest R^2 while the Banki had the lowest. The paddy cultivar on which the model best fitted the experimental drying data was based on lowest RMSD and highest R^2. The Banki cultivar had the lowest RMSD, showing that the model better tracked its experimental data points while the De-gold with the highest R^2 showed that the model prediction curve followed more closely the trend of its drying curve.

Drying Characteristics of Parboiled Paddy Cultivars

The variation of the predicted and observed moisture ratios with time for parboiled Banki, De-gold, and Liberia paddy cultivars is presented in Fig. 8. This figure shows that the moisture ratio of the cultivars decreased with increase in time. Towards the end of the drying process, the trend tended to become asymptotic to the time axis.

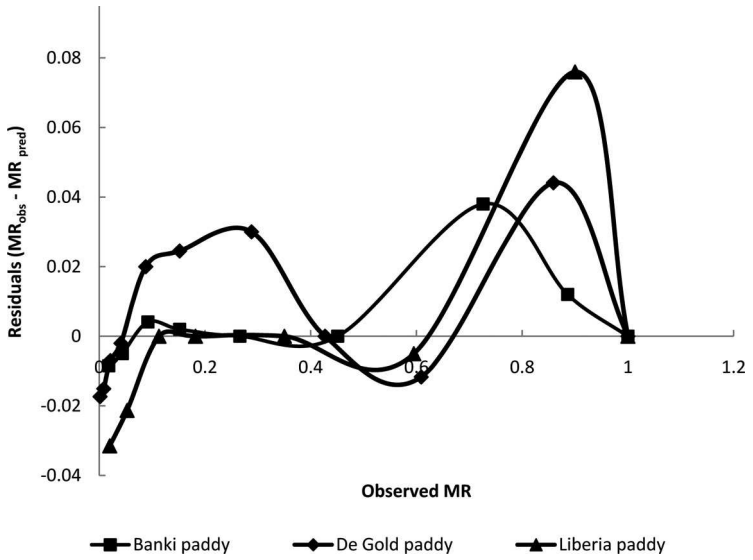


FIG. 7. Moisture ratio residual plots for parboiled Banki, De Gold, and Liberia paddy cultivars.

Downloaded by [Ndubisi Aviara] at 10:28 05 April 2013

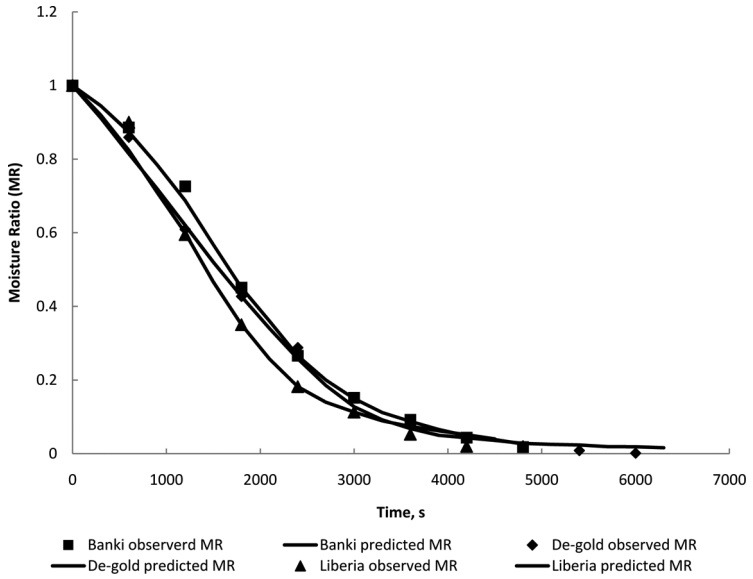


FIG. 8. Variation of predicted and observed moisture ratios with time for different parboiled paddy cultivars dried at 60°C.

Downloaded by [Ndubisi Aviara] at 10:28 05 April 2013

The figure also shows that the model closely predicted the observed moisture ratios of the samples at the drying temperature of 60°C.

Reliability of the Drying Model

The reliability of the model for describing the drying curves of the paddy samples was evaluated by comparing the predicted moisture ratios of the samples with those obtained experimentally. The predicted moisture ratios were plotted against the observed moisture ratios. A model is considered reliable if the predicted moisture ratios fall near the line $y = x$.[48] Figure 9 shows that the predicted moisture ratios of the Banki, De-Gold, and Liberia cultivars banded around a straight line with high R^2, indicating that the model tracked well the drying curves of these paddy cultivars throughout their drying period. This further proves that the developed model was suitable for use in describing the drying behavior of the parboiled paddy cultivars.

The variations of the drying rate of parboiled paddy cultivars with time and moisture content are shown in Figs. 10 and 11, respectively. The constant drying rate period was not observed, as was the case in the findings of Igathinathane and Chattopadhyay.[7] Drying rate varied with paddy cultivar though the initial moisture content was not uniform. For each cultivar, there existed an induction period followed by two distinct falling rate periods, which comprised an initial period that occurred as the moisture

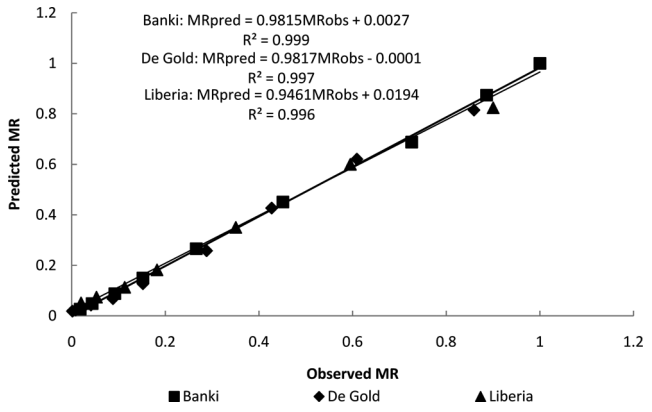


FIG. 9. Plots of predicted against observed moisture ratios of parboiled Banki, De Gold, and Liberia paddy cultivars.

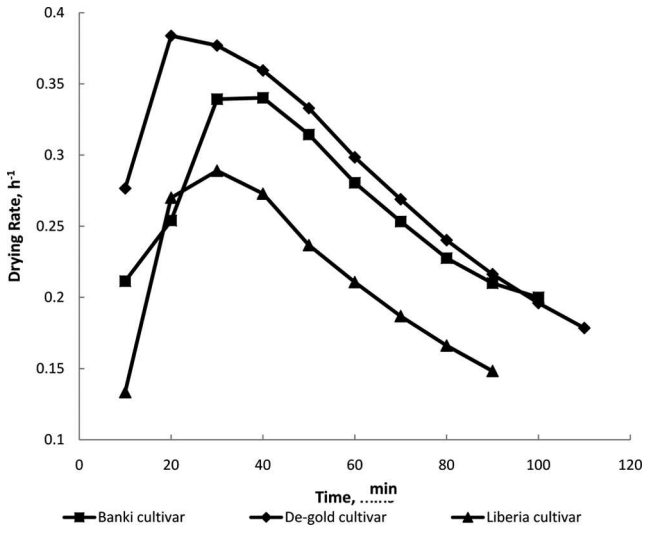


FIG. 10. Variation of the drying rate with time for different parboiled paddy cultivars dried at 60°C.

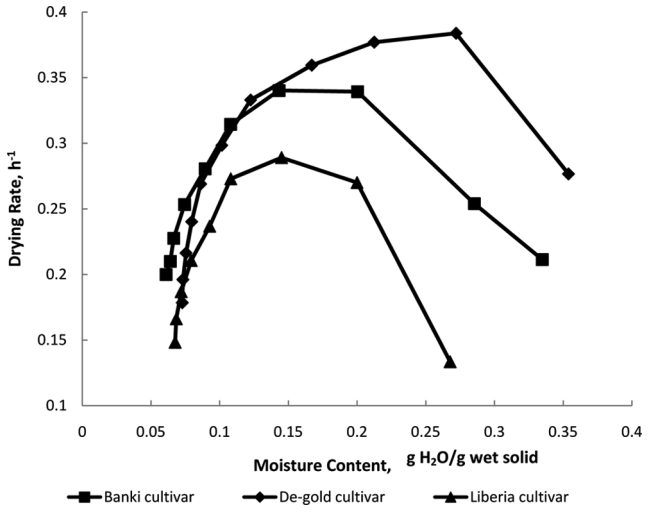


FIG. 11. Variation of the drying rate with moisture content for different parboiled paddy.

content decreased from 17 to 9% for Banki, 25 to 12% for De-gold, and 15 to 9.5% for Liberia, and a second but slower one that occurred over the remaining range of moisture decrease. A similar observation was reported by Ng et al.[53] on Malaysian paddy. The cultivars exhibited critical moisture content, which was found to be 17%, 25%, and 15% on a wet basis for Banki, De-gold, and Liberia, respectively.

CONCLUSIONS

From the results of this study, the following conclusions were drawn:

1. The average length, width, and thickness of parboiled paddy cultivar at the moisture contents of 37.14% for Banki, 40% for De-gold, and 29.28% for Liberia were 9.86, 2.59, and 2.02 mm; 11.21, 2.70, and 2.13 mm; and 8.32, 2.88, and 2.03 mm, respectively.
2. The equivalent diameter of the Banki, De-gold, and Liberia was 3.73, 4.75, and 3.68 mm, respectively.
3. The prolate spheroidal geometric dimensions of equatorial and polar radii were 1.16 and 4.78 mm, 1.22 and 5.45 mm, and 3.10 and 3.92 mm for Banki, De-gold, and Liberia, respectively.
4. Moisture diffusion coefficient was cultivar-dependent.
5. Drying of the parboiled paddy cultivars occurred in the falling rate phase with initial period of induction and critical moisture content that varied with cultivar.
6. The mathematical model developed for predicting moisture transport during the drying of parboiled paddy based on the prolate spheroidal coordinate system and paddy effective moisture diffusivity adequately simulated the drying process.
7. Application of the prolate spheroidal coordinate system reduced the simulation to a one-dimensional model.
8. Comparison of the experimental and predicted moisture ratios showed low root mean square deviation and high coefficient of determination for all the cultivars.
9. Model predictive capacity was parboiled paddy-cultivar-dependent.

REFERENCES

1. USDA. *Rice Area, Yield, and Production.* USDA Foreign Agricultural Service. Available at http://www.fas.usda.gov (accessed May 11, 2010).
2. Otegbayo, B.O.; Osamue, F.; Fashakin, J.B. Effect of parboiling on physio-chemical qualities of two local rice varieties in Nigeria. *The Journal of Food Technology in Africa* **2001**, *6*(4), 130–132.
3. Ibukun, E.O. Effect of prolonged parboiling duration on proximate composition of rice. *Scientific Research and Essay* **2008**, *3*(7), 323–325.
4. Sareepuang, K.; Siriamornpun, S.; Wiset, L.; Meeso, N. Effect of soaking temperature on physical, chemical and cooking properties of parboiled fragrant rice. *World Journal of Agricultural Sciences* **2008**, *4*(4), 409–415.
5. Miah, M.A.K.; Haque, M.A.; Douglass, P.; Clarke, B. Parboiling of rice. Part II: Effect of hot soaking time on the degree of starch gelatinization. *International Journal of Food Science and Technology* **2002**, *37*, 539–545.
6. Bakshi, A.S.; Singh, R.P. Drying characteristics of parboiled rice. In *Drying '80*; Majumdar, A.S.; Ed. Hemisphere Publishing Corporation: New York, 1980; 282–288.
7. Igathinathane, C.; Chattopadhyay, P.K. Moisture diffusion modelling of drying in parboiled paddy components. Part I: Starchy endosperm. *Journal of Food Engineering* **1999**, *41*(2), 79–88.
8. Likitrattanaporn, C.; Noomhorm, A. Effects of simultaneous parboiling and drying by infrared radiation heating on parboiled rice quality. *Drying Technology* **2011**, *29*(9), 1066–1075.
9. Igathinathane, C.; Chattopadhyay, P.K. Moisture diffusion modelling of drying in parboiled paddy components. Part II: Bran and husk. *Journal of Food Engineering* **1999**, *41*(2), 89–101.
10. Steffe, J.F.; Singh, R.P. Liquid diffusivity of rough rice components. *Transactions of the ASAE* **1980**, *23*(3), 767–774, 782.
11. Aguerre, R.J.; Suarez, C. Viollaz, P.E. Drying kinetics of rough rice grain. *Journal of Food Technology* **1982**, *17*, 679–686.
12. Lague, C. Modeling pre-harvest stress-cracking of rice kernels. Ph.D. thesis, University of California, Davis, USA, 1990.
13. Sarker, N.N.; Kunze, O.R.; Strouboulis, T. Finite element simulation of rough rice drying. *Drying Technology* **1994**, *12*(4), 761–775.
14. Prakash, B.; Pan, Z. Heat and mass transfer modeling of rough rice under convective and infrared drying. *ASAE Paper*, No. 096420, St. Joseph, USA, 2009.
15. Suarez, C.; Viollaz, P.E.; Chirife, J. Diffusional analysis of air drying of grain sorghum. *Journal of Food Technology* **1980**, *15*, 523–531.
16. Steffe, J.F. Singh, R.P. Diffusivity of starchy endosperm and bran of fresh and rewetted rice. *Journal of Food Science* **1980**, *45*, 356–361.
17. Aguerre, R.J.; Suarez, C.; Viollaz, P.E. Analysis of the interface conditions during drying of rice. *Journal of Food Technology* **1984**, *19*, 315–323.
18. Haghighi, K.; Segerlind, L.J. Modeling simultaneous heat and mass transfer in an isotropic sphere – A finite element approach. *Transactions of the ASAE* **1988**, *31*(2), 629.
19. Brooker, D.B.; Bakker-Arkema, F.W.; Hall, C.W. *Drying of Cereal Grains*; The AVI Publishing Company Inc.: Westport, CT, 1992.
20. Crank, J. *The Mathematics of Diffusion*, 2nd Ed; Oxford Science Publications: New York, 1992.

Downloaded by [Ndubisi Aviara] at 10:28 05 April 2013

21. Gebhart, B. *Heat Conduction and Mass Diffusion*, 2nd Ed; McGraw-Hill Inc.: New York, 1993.
22. Lima, D.R.; Farias, S.N.; Lima, A.G.B. Heat and mass transfer inside oblate and prolate spheroids: An exact solution. In *Drying 2004 – Proceedings of the 14th International Drying Symposium (IDS 2004)*, São Paulo, Brazil, August 22–25, 2004, vol. A: 493–500, 2004.
23. da Silva, W.P.; e Silva, C.M.D.P.S.; do Nascimento, P.L.; e Silva, D.D.P.S.; e Silva, C.D.P.S. Influence of the geometry on the numerical simulation of isothermal drying kinetics of bananas. *World Applied Sciences Journal* **2009**, *7*(7), 846–855.
24. da Silva, W.P.; e Silva, C.M.D.P.S.; Farias, V.S.O.; Gomes, J.P. Diffusion models to describe the drying process of peeled bananas: Optimization and simulation. *Drying Technology* **2012**, *30*(2), 164–174.
25. de Lima, A.G.B.; Nebra, S.A. Theoretical analysis of the diffusion process inside prolate spheroidal solids. *Drying Technology* **2000**, *18*(1 & 2), 21–38.
26. de Oliveira, V.A.B.; de Lima, A.G.B. Mass diffusion inside prolate spherical solids: An analytical solution. *Revista Brasileira de Produtos Agroindustriais, Campina Grande* **2002**, *4*(1), 41–50.
27. Carmo, J.E.F.; Lima, A.G.B. Mass transfer inside oblate spheroidal solids: Modelling and simulation. *Brazilian Journal of Chemical Engineering* **2008**, *25*(1), 19–26.
28. Igathinathane, C.; Chattopadhyay, P.K.; Pordesimo, L.O. Moisture diffusion modeling of parboiled paddy accelerated tempering process with extended application to multi-pass drying simulation. *Journal of Food Engineering* **2008**, *88*, 239–253.
29. Prakash, B.; Pan, Z. Effect of geometry of rice kernels on drying modeling results. *Drying Technology* **2012**, *30*(8), 801–807.
30. Lu, R.; Siebenmorgen, T.J. Moisture diffusivity of long-grain rice components. *Transactions of the ASAE* **1992**, *35*(6), 1955–1961.
31. de Elvira, C. The use of alternating direction implicit methods to model diffusion phenomena in elliptic products. *Journal of Food Engineering* **1993**, *19*, 159–170.
32. Sokhansanj, S.; Gustafson, R.J. Prediction of heat and mass transfer within a grain kernel - A finite element application. In *Drying '80*; Majumdar, A.S.; Ed. Hemisphere Publishing Corporation: New York, 1980; 229–232.
33. Aguerre, R.J.; Suarez, C. Numerical analysis of the diffusion equation for composite solids: Application to grain drying. *Journal of Food Engineering* **1992**, *17*, 201–215.
34. Muthukumarappan, K.; Gunasekaran, S. Moisture diffusivity of corn kernel components during adsorption. Part III: Soft and hard endosperms. *Transactions of ASAE* **1994**, *37*, 1275–1280.
35. Igathinathane, C.; Chattopadhyay, P.K. Mathematical prediction of moisture profile in layers of grain during preconditioning. *Journal of Food Engineering* **1997**, *31*, 185–197.
36. Raffie, S.; Keyhani, A.; Mohammadi, A. Soybean seeds mass transfer simulation during drying using finite element method. *World Applied Sciences Journal* **2008**, *4*(2), 284–288.
37. Janas, S.; Boutry, S.; Malumba, P.; Elst, L.V.; Bera, F. Modelling dehydration and quality degradation of maize during fluidized bed drying. *Journal of Food Engineering* **2010**, *100*, 527–534.
38. Igathinathane, C. Studies on drying and tempering of parboiled paddy and development of mathematical models for the processes. Ph.D. thesis, Indian Institute of Technology, Kharagpur, India, 1997.
39. Kreyszig, E. *Advanced Engineering Mathematics*, 8th Ed; John Wiley & Sons Inc.: New York, 1999.
40. Shyamali, A.K.; Jayaweera, H.H.E.; Ariyaratne, T.R. Thin-layer drying of some Sri Lankan paddy varieties under low humid conditions. *Proceedings of the Technical Sessions, Institute of Physics – Sri Lanka* **2009**, *25*, 36–44.
41. Rao, S.P.; Bal, S.; Goswami, T.K. Modelling and optimization of drying variables in thin layer drying of parboiled paddy. *Journal of Food Engineering* **2007**, *78*, 480–487.
42. Carnahan, B.; Luther, H.A.; Wilkes, J.O. *Applied Numerical Methods*; John Wiley & Sons Inc.: New York, 1969.
43. Veerarajan, T.; Ramachandran, T. *Numerical Methods*, 2nd Ed; Tata McGraw-Hill Publishing Company: New Delhi, 2007.
44. Senadeera, W.; Bhandari, B.R.; Young, G.; Wijesinghe, B. Influence of shapes of selected vegetable materials on drying kinetics during fluidized bed drying. *Journal of Food Engineering* **2003**, *58*, 277–283.
45. Aviara, N.A.; Mamman, E.; Umar, B. Some physical properties of Balanites Aegyptiaca nuts. *Biosystems Engineering* **2005**, *92*(3), 325–334.
46. Reddy, B.S.; Chakraverty, A. Physical properties of raw and parboiled paddy. *Biosystems Engineering* **2004**, *88*(4), 461–466.
47. Kibar, H.; Ozturk, T.; Esen, B. The effect of moisture content on physical and mechanical properties of rice (*Oryzasativa* L.). *Spanish Journal of Agricultural Research* **2010**, *8*(3), 741–749.
48. Syarief, A.M.; Morey, R.V.; Gustafson, R.J. Thin layer drying rates of sun flower seed. *Transactions of the ASAE* **1984**, *27*, 195–200.
49. Ajibola, O.O. Thin layer drying of melon seed. *Journal of Food Engineering* **1989**, *9*, 305–320.
50. Ajibola, O.O.; Aviara, N.A.; Abodunrin, V.K. Moisture sorption equilibrium and thermodynamic properties of palm kernel. *International Agrophysics* **2005**, *19*, 273–283.
51. Li, X.J.; Wu, Z.D.; Zhang, Z.J.; Lu, H.; Lin, J.Y.; Cao, Y. The sorption isosteric heats of rice grains in China. In *10th International Working Conference on Stored Product Protection, Julius-Kühn-Archive, Academy of the State Administration of Grains*, Beijing, China, 2010.
52. Madamba, P.S.; Driscoll, R.H.; Buckle, K.A. The thin-layer drying characteristics of garlic slices. *Journal of Food Engineering* **1996**, *37*, 437–449.
53. Ng, P.P.; Law, C.L.; Tasirin, S.M. Drying kinetics of Malaysian paddy (Group D Particles) in spouted bed dryer. *International Journal of Food Engineering* **2006**, *2*(3), Article 1.

Downloaded by [Ndubisi Aviara] at 10:28 05 April 2013